# Material Development for Supercritical Water-cooled Reactor

**J. Kaneda[1], S. Kasahara[1], F. Kano[2], N. Saito[2], T. Shikama[3] and H. Matsui[4]**
[1] Materials Research Laboratory, Hitachi, Ltd., Hitachi, Ibaraki, Japan
[2] Power and Industrial Systems R&D Center, Toshiba Corp., Yokohama, Kanagawa, Japan
[3] Institute for Materials Research, Tohoku University, Oarai, Ibaraki, Japan
[4] Institute of Advanced Energy (IAE), Kyoto University, Gokanosho Uji-shi, Kyoto, Japan

## Abstract

Material properties of candidate alloys, including ferritic/martensitic steels, austenitic stainless steels, Ni based alloys, Ti alloys have been investigated to evaluate their applicability for fuel claddings of the supercritical water-cooled reactor (SCWR) in Japanese national projects since 2000. Modified austenitic stainless steels such as fine grain materials and Zr-modified materials have also been investigated. In the projects, high temperature tensile tests, creep tests, general corrosion tests, stress corrosion cracking (SCC) tests, and manufacturability tests were conducted under the predicted conditions in the SCWR. The following results were obtained from the tests. Several of the test materials satisfied the tensile properties required for the fuel cladding design. Requirement of the creep rupture lifetime is 50,000 h under 30 – 50 MPa at 700˚C. Several materials such as alloy 625, type 310S and Zr-modified type 316L and type 310S were expected to meet the design requirements. Ni based alloys, type 310S, Zr-modified type 310S and the fine grain materials had good general corrosion resistance. SCC did not appear in any test materials except type 304, 310S, Ti alloy and Alloy 625. Austenitic stainless steels could be manufactured by the process proven for the seamless tube with about 4.5 mm in outside diameter. Alloy 690 and the fine grain material could be manufactured with a minor process modification as well. According to the calculation of He yield, He embrittlement is a serious concern for Ni-based alloys because of their the high Ni content. As a result of the comprehensive evaluation, Zr-modified type 310S is the first candidate alloy, and Ti-modified type 310S is the second candidate alloy for the JSCWR fuel rod. Considering the standard of mechanical design, the existing material is favorable to be considered for the power plants. Thus, type 310S with reduced carbon content within the alloy specification is recommended as the second candidate material.

## 1. Introduction

Supercritical water-cooled reactor (SCWR) is expected to be a promising future nuclear power system with considerably higher thermal efficiency and smaller specific volume than conventional light water reactors (LWRs). Material selection for core components, in particular fuel claddings, is thought to be a key factor for the viability of the SCWR, since severe environment is predicted including a wide temperature range and a high dose of neutron irradiation. For materials in conventional LWRs, both of corrosion resistance and neutron irradiation resistances are required. Similarly, fast breeder reactors (FBR) require not only the performance of high temperature strength but also neutron irradiation resistance for the reactor core materials, whereas supercritical pressure fossil power (SCFP) and supercritical water oxidation (SCWO) systems also required corrosion resistance and high temperature strength. Under the operating conditions of an SCWR, the concurrent requirements of irradiation resistance, corrosion resistance and high-temperature strength must be fulfilled, which has not been experienced before in the existing industry. From this perspective, it can be understood that finding materials applicable for the SCWR core condition is an essential task in the SCWR development.

In this context, material studies were carried out from Japanese fiscal year (FY)2000 to FY2010 as three parts of the Japanese SCWR (JSCWR) development project that consisted of system design, heat transfer and material screening, and which was supported by the Institute of Applied Energy (IAE) / the Ministry of Economy, Trade and Industry (METI)[1,2]. In these projects, the fuel rod behaviour was evaluated based on the plant specification in which the average temperature of coolant at the reactor core exit was estimated to be 560˚C or higher and the maximum temperature of the fuel cladding surface was estimated to be 700˚C or lower. Fuel behaviour analyses [3] show that mechanical strength and creep properties especially at high temperatures have a great influence on the integrity of the fuel rod. To combine the integrity of the fuel rod with the economy of the fuel cycle, the corrosion characteristics of the cladding by the supercritical water coolant become a very important factor in the fuel design. These required specifications were incorporated into the material testing from the view point of the fuel design, based on this fuel behaviour analysis and the view point of what data had to be acquired during the material testing. Based on these evaluation results, the requirements for the materials were provided. Table 2 shows the required specifications for material tests.

The purpose of the development projects was to identify the material that can be used even under the severe conditions of neutron irradiation at high temperatures in the corrosive environment of supercritical water (SCW). A wide variety of test materials were chosen from commercial alloys and modified alloys, considering the materials for existing nuclear and chemical industries such as LWR, FBR, SCFP and SCWO. Through the survey on the requirements for the reactor core materials, the test items, test conditions and criteria were determined in terms of the mechanical properties, phase stability, corrosion behaviour, and SCC properties after irradiation. Furthermore, He embrittlement needs to be considered for materials to be used in the components under a high fluence of neutron irradiation. The He yield was calculated taking into account of the transmutation reactions.

The authors evaluated whether the material performance satisfies the design requirements by comparing experimental data with the design requirements. If the material performance does not meet the design requirements, it is necessary to revise the system design or to improve the material performance.

## 2. Test Materials

Zirconium alloys (Zircaloy-2 and Zircaloy-4) are widely used for LWR fuel claddings, but it is difficult to use them for the JSCWR, mainly because the tensile strength of Zircaloys is very low above 400°C. Therefore, alternative alloys need to be developed for the JSCWR fuel claddings.

Test materials were selected from austenitic stainless steels, high chromium containing ferritic/martensitic steels (F/M steels), Ni-based alloys and Ti-based alloys using a previous data survey of the literature. These materials have been used for the existing components of supercritical and ultra supercritical (USC) fossil fired power plants [4] and SCWO systems for hazardous waste destruction. Austenitic stainless steels and F/M steels are mainly used as tubes, pipes and turbine components in USC power plants. In SCWO systems, hazardous wastes can be oxidized to acidic products. Such acidic conditions may result in significant corrosion of the process units. For this reason, it is desirable that highly corrosion-resistant materials, such as Ni-based alloys and Ti-based alloys, are used for SCWO system components. On the other hand, nuclear materials have been developed to reduce the damage due to neutron irradiation for the core components and structures of LWRs, fast reactors (FRs) and fusion reactors. One of the major issues in radiation damage is swelling, and efforts have been made to reduce it. In particular, austenitic stainless steels are highly sensitive to swelling under relatively high temperature irradiation conditions. Special stainless steels have been developed and used for the fuel claddings and core components of FRs. The above-mentioned technical information was very important not only to target test materials and facilitate examinations at the beginning of the material screening, but also to minimize the time and cost for the development. Therefore, test materials were selected from commercially available materials, with consideration of data from the USC, SCWO and nuclear fields.

For application in a JSCWR core environment, the candidate materials must be resistant to corrosion and radiation damage, and have good mechanical properties at high temperatures. Austenitic stainless steels modified with the addition of zirconium, which has the effect of suppressing vacancy migration, to improve radiation damage resistance have been developed. Focusing on the corrosion performance and mechanical properties, a fine grain stainless steel (denoted by “F” in the present paper) was developed for JSCWR core component material. T3F, T3N, T6F, T6N are in the same family, which was modified from type 310S with Ti addition and grain control by cold work and recrystallization heat treatment.

Selected materials in this technical development are shown in Table 3. Solution heat treatment (SHT) was done on most of them, and some were further heat treated under designated conditions after SHT. Conditions are shown in Table 3. After the heat treatment, materials were machined into specimens.

## 3. Experimental Procedure

### 3.1 Tensile test

In the planned design of the SCWR, the outlet coolant temperature is 560°C. Thus, tensile tests were carried out at room temperature and 550°C in air. The strain rate used for the tensile testing was $5x10^{-3}$ $s^{-1}$.

### 3.2 Creep test

Based on the preliminary analysis of the stress on the fuel cladding, the creep rupture lifetime of fuel cladding materials should be more than 50,000 h under 30 - 50MPa of stress at 700°C. Thus, to predict the creep rupture lifetime at 700°C, creep rupture tests were carried out under loading conditions at 700°C and 800°C.

## 3.3 General corrosion test

The general corrosion tests were carried out on coupon-shaped specimens (Figure 6). Four coupon specimens for each material were immersed as a set in supercritical water. The general corrosion test conditions were as follows:

- Temperatures: 290, 380, 500, 550, and 600°C
- Pressure: 25 MPa
- Dissolved oxygen concentration: 8 ppm
- Conductivity: less than 0.1 μS/cm
- Exposure time: up to 1000 hours.

The general corrosion properties were evaluated using the weight change measured before and after the test. The weight measurement was carried out using a sensitive electronic balance. The accuracy of the weight measurement was ±0.01 mg.

For this test, the weight change of materials included the weight that increased due to the growth of the oxide film and the weight that decreased due to the loss of materials. Generally, general corrosion behaviour was evaluated by the amount of weight by which materials changed. However, for materials that have exfoliation of the oxide film, general corrosion behaviour of these materials could not be evaluated by using only the amount of weight by which they had increased. Therefore, in this study, after the weight measurement was finished, the oxide film from the specimen was removed using molten lithium. The temperature of molten lithium was selected as 600℃, which is close to the highest general corrosion test temperature in this research. Finally the weight loss was measured as the difference in weight of the same specimen before and after the corrosion test without oxide film.

## 3.4 SCC test

The SCC susceptibility was evaluated with slow strain rate test (SSRT). The SSRT test conditions were as follows:

- Temperatures: 290 and 550°C
- Pressure: 25 MPa
- Dissolved oxygen: 8 ppm
- Strain rate: $4x10^{-7}$ $s^{-1}$

## 3.5 Manufacturability

The manufacturability of the small-diameter and thin-wall tube was examined for the selected alloys through trial tests in the factory where the fuel cladding tube is manufactured. The manufacturing process is shown in Figure 7. The pierced raw pipe with 17.0 mm-outer diameter (OD), 12.0 mm-inner diameter (ID), 2.5 mm-thickness and 170 mm-length was drawn to 12.2 mm-OD in the first step. Then intermediate annealing and drawing rolling were repeated three times for austenitic stainless steels and five times for nickel-base alloy. Annealing was executed at 980°C for the fine-grained alloys and at 1100°C for other alloys. After final annealing, straightening and polishing were carried out to attain the projected outer diameter of 4.57 mm and thickness of 0.25 mm. Microstructure was inspected with an optical microscope to evaluate the integrity of tube production.

# 4. Test Results

## 4.1 Tensile test [5, 6]

All of the test materials were examined to obtain their mechanical properties at room temperature and 550°C. Fuel cladding was designed using the mechanical properties of type 316 SS. In this section, tensile properties of the test materials are compared with that of type 316 SS. Tensile strength and total elongation, which were analysed from stress-strain curves, are shown in Figure 8. Generally, tensile strength decreased with increasing test temperature. Austenitic stainless steels such as type 316L and 310S had similar tensile properties to type 316 SS as well as modified austenitic stainless steels. F/M steels had higher strength and lower elongation compared with austenitic stainless steels. Tensile strength and total elongation of Ni base alloys are higher than those of stainless steels, especially at high temperature. Alloy 718 showed the highest tensile strength among stainless steels and Ni base alloys. Alloy 718 with ordinary thermal treatment (alloy 718 (ordinary)) is one of the precipitate hardening alloys; therefore, the tensile strength at 550°C is thought to be attributed to precipitates in the matrix. Total elongation of alloy 718 was low compared with other stainless steels and Ni base alloys.

Ti-based alloys had high yield and tensile strengths compared with type 316SS at both high and low temperature. Ti-15Mo-5Zr-3Al showed the highest tensile strength among the Ti alloys, but the strength was almost halved at 550°C. The other titanium alloys also showed higher strength than stainless steels at room temperature, but the tensile strength at 550°C decreased significantly compared with the other alloys. Furthermore, Ti alloys showed low total elongation among the tested materials not only at room temperature but also at 550°C. In the case of Ti alloys, the temperature dependence of the mechanical property change was significantly different from other alloys.

## 4.2 Creep test [7, 8]

Figure 9 shows the relationship between creep rupture lifetime and stress of Zr-modified stainless steels at 700°C and 800°C under uniaxial load along with NIMS creep data of type 316H TB at 700°C [8,9]. Fitting was performed using the Larson-Miller parameter, and the following approximate expression was obtained:

$$\log t_R = \frac{b_0 + b_1(\log\sigma) + b_2(\log\sigma)^2}{T + 273.15} - C \qquad (1),$$

where $t_R$ is creep rupture time, $\sigma$ is stress, $T$ is temperature and $b_0$, $b_1$, $b_2$ and $C$ are constants. Table 4 shows coefficients and constants obtained by fitting. The relationship between stress and creep rupture life time based on the approximate expression is shown in Figure 9. The stresses at which the creep rupture lifetime exceeds 50,000 h were 47.4 MPa for H1 (type316L+Zr) and 36.2 MPa for H2 (type310S+Zr). If the stress is below these stresses for each Zr-modified stainless steel, a creep rupture lifetime of 50,000 h may be attained. This suggests that the target creep rapture lifetime of 50,000 h under 30 - 50MPa of stress at 700 °C can be achieved.

Figure 10 shows the rupture time as a function of applied stress by thermal creep at 700°C obtained by the uniaxial test and pressurized tube tests, where the results of the tube test are represented by larger symbols. The stress for tube tests are converted by von Mises equivalent stress. Dashed lines show estimated lifetime using the Larson-Miller Parameter (LMP), based on the stress-rupture time relation at 700°C and 800°C. H1, H2, T6N, type 310S and Alloy 625 are expected to satisfy the design requirement from the estimation of the creep rupture stress for 50,000 hours. The results of uniaxial tests and pressurized tube tests were in good agreement, which shows the suitability of this method for irradiation tests.

## 4.3 General corrosion test [6, 7, 10-22]

Figure 11 shows the weight changes of the test materials as a function of temperature. The weight changes of type 310S and the Ni-based alloys were very small and some of them showed weigh loss. The weight changes of type 316L and 304 were larger than these of type 310S at 550°C. The weight changes of Ti-15V-3Al-3Sn-3Cr and Ti-15Mo-5Zr-3Al were about the same as those of type 316L and type 304. On the other hand, the weight changes of Ti-6Al-4V and Ti-3Al-2.5V were smaller than HCM12, the F/M steel, but were still large.

Figure 12 shows the weight change of the materials exposed for 1000h in supercritical water at 500, 550, and 600°C. Each datum is the average weight change of four specimens. The weight changes of type 304, type 316L, H1 (modified Type316L), and 12Cr-1Mo-1WVNb increased along with the test temperature. The weight changes of 600°C of type 304, type 316L, and H1 decreased compared with the results of those at 500 and 550°C. Generally, weight change occurs according to the oxidization of materials, so it is thought that the weight of specimens will increase with increasing test temperature. In the case of Type 304, Type 316L, and H1, exfoliation of the oxide film of these materials occurred under 600°C supercritical water conditions. However, the weight change of these materials depended on the oxidization of the materials. On the other hand, the weight changes of T3F and T7F (fine grain Type 310S) decreased along with the test temperature. For T3F and T7F, the exfoliation of oxide film was not observed. Therefore dissolution of these materials was more dominant than oxidation. In these results, type 310S and modified type 310S (H2, T3F, T7F) had smaller weight changes than other materials. Alloy 600 and 625 had similar good general corrosion performance comparable as H2. Alloy 690 seemed to have a good general corrosion resistance but the weight loss increased with temperature.

To remove the oxide film from these specimens, the general corrosion specimens after a corrosion tests were immersed in 600°C molten lithium, and the weight changes after immersion were measured. The amount of weight loss was evaluated by using the following formula:

$$\Delta W = \left(W_0 - W_{removal}\right) / S \tag{2}$$

$W_0$: Specimen weight before the general corrosion test
$W_{removal}$: Specimen weight after the removal process
$S$: Surface area of specimen

Figure 13 shows the relationship between the logarithms of the amount of weight loss and the reciprocal of the test temperature. Every material indicated a good linear relationship on the Arrhenius plot.

Generally, the growth rate of an oxide film tends to depend on the diffusion rate of the metal element and the oxygen. Therefore, this research predicted the relationship between weight loss ($\Delta W$) and test temperature using the following formula:

$$\Delta W = A_0 \exp\left(-\frac{E}{kT}\right) \quad (3)$$

$A_0$: Constant
$E$: Apparent activation energy
$k$: Boltzmann constant
$T$: Absolute temperature

Meanwhile, the time dependence of weight loss is generally given by the following formula:

$$\Delta W = C_0 t^n \quad (4)$$

$C_0$: Constant
$t$: Time
$n$: Exponent

Although it depends on the test conditions, the value of n is usually 1/3-1/2. In this case, the value of n was set to 1/2. The predicted results of the depth of corrosion thinning at 700 °C for 50,000h are shown in Table 4. The depth of corrosion thinning of Type 304 was 570 µm, that of type 316L was 720 µm, that of 12Cr-1Mo-1WVNb was 820 µm, and that of H1 was 1160 µm. These values were larger than the thickness of fuel claddings. On the other hand, the depth of corrosion thinning of Type 310S was 27 µm, that of H2 was 42 µm, that of T3 was 35 µm, and that of T7 was 14 µm. These values were smaller than 1/10 of the thickness of fuel claddings. Based on the above results, Type 310S and modified Type 310S were the most promising alloys for the fuel cladding.

### 4.4 SCC test [13, 14]

The SCC susceptibility was evaluated using slow strain rate test (SSRT). The results of the SSRTs are shown in Table 5. The sensitized type 304 SS had SCC cracks at 290°C but SCC susceptibility tended to decrease with test temperature. SCC cracks appeared in type 310S SS at both 290 and 550°C. Alloy 690 had SCC cracks only at 550°C. Ti-15Mo-5Zr-3Al also had significant SCC cracks at 550°C. There was no SCC crack in type 316L, HCM12, alloy 600, alloy 625, H2 and T6F, which had good SCC resistivity. Although H2 is a type 310S-derived material, H2 had good SCC resistance whereas type 310S had SCC susceptibility. H2 has low carbon content and zirconium alloying element compared with type 310S. Chromium depletion due to carbide formation is thought to be one of the major causes of intergrannular SCC. Therefore, if the carbon content is sufficiently reduced in type 310S, the SCC resistance would be improved even without zirconium. This can be done within the composition range defined for type 310S stainless steel, without violating the standard.

## 4.5 Manufacturability ]15]

The manufacturability was examined for the small diameter, thin-wall tubes with 2000 mm-length and the projected outer diameter and thickness of 4.57 mm and 0.25 mm. The resulting product of each material exhibited sufficient manufacturability, although the thicknesses slightly exceeded the target value as follows:

/ Type 316L: 4.564 mm OD, 0.279-0.292 mm t
/ Type 310S: 4.567 mm OD, 0.280-0.297 mm t
/ T6F: 4.567 mm OD, 0.279-0.292 mm t
/ H1: 4.561 mm OD, 0.295-0.313 mm t
/ H2: 4.566 mm OD, 0.279-0.292 mm t
/ Alloy 690: 4.565 mm OD, 0.281-0.321 mm t

Microstructures of the tubes are shown in Figure 14. No notable irregularity of microstructure was observed. Thus, the fuel rod could be manufactured with type 316L, 310S, T6F, H1, H2 and alloy 690.

## 4.6 He generation

Table 8 shows the amount of He yield calculated with Greenwood's equation[16], taking account of the transmutation reactions of $^{58}Ni(n,\gamma)^{59}Ni(n,\alpha)^{56}Fe$, $^{58}Ni(n,\alpha)^{55}Fe$ and $^{60}Ni(n,\alpha)^{57}Fe$ at the neutron fluence of $8\times10^{21}$ n/cm$^2$, using the neutron energy spectrum obtained in this project[10]. The amount of He increases with Ni content and it turned out to be roughly threefold in alloy 690 as compared with that in type 316L. Based on these results, He embrittlement is a serious concern for Ni-based alloys because of their high Ni content. It seems difficult to use Ni-based alloys for fuel rods in mixed spectrum reactors including JSCWR.

# 5. Conclusion

Selected test materials were investigated in terms of their material properties under the predicted conditions in the SCWR. The following results were obtained through the tests. Several of the test materials satisfied tensile properties required for the fuel cladding design. The requirement for creep rupture lifetime is 50,000 h under 30 – 50 MPa at 700°C. Several materials such as alloy 625, type 310S and Zr-modified type 316L and type 310S were expected to meet these design requirements. Ni based alloys, type 310S, Zr-modified type 310S and the fine grain materials had good general corrosion resistance. SCC did not appear in any test materials except type 304, 310S, Ti alloy and alloy 625. Austenitic stainless steels could be manufactured using the proven process for the seamless tube with about 4.5 mm in outside diameter. Alloy 690 and the fine grain material could be manufactured with a minor process modification as well. He embrittlement is a serious concern for Ni-based alloys. Figure 21 shows the results of the comprehensive evaluation of the test materials. In the evaluation, Zr-modified type 310S(H2) is selected as the first candidate alloy, and Ti-modified type 310S is the second candidate alloy for the JSCWR fuel rod. For immediate applications, e.g. the EU Fuel Qualification Test, code-qualified alloys have definite advantages in terms of qualifying the material by the relevant code and specifications. For this purpose, type 310S stainless steel with reduced carbon content within the composition range defined in the standard is also recommended as a candidate material.

## 6. References

[1] A. Shioiri, K. Moriya, Y. Oka, H. Mori, H. Takahashi, Development of Supercritical-water Cooled Power Reactor Conducted by a Japanese Joint Team," GENES4/ANP2003, Paper 1121, Kyoto, Japan, September 15-19, 2003.

[2] Y. Oka and K. Yamada, "Research and Development of High Temperature Light Water Cooled Reactor Operating at Supercritical-Pressure in Japan," Proc. ICAPP'04, Paper 4233, Pittsburgh, USA, June 13-17, 2004.

[3] Toshiba Corporation, Hitachi, Ltd., Tohoku University and The University of Tokyo, "Development of Materials for Supercritical-Water-Cooled Reactor (SCWR)," Interim report of Innovative and Viable Nuclear Energy Technology (IVNET) Development Project (2005), (in Japanese).

[4] J. Matsuda, N Shimono and K. Tamura, "Supercritical Fossil Fired Power Plants Designs and Developments" ibid. Paper No. 107.

[5] S. Kasahara, J. Kuniya, K. Moriya, N. Saito, S. Shiga, "General Corrosion of Iron, Nickel and Titanium Alloys as Candidate Materials for the Fuel Claddings of the Supercritical-water Cooled Power Reactor," GENES4/ANP2003, Paper 1132, Sep. 15-19, 2003, Kyoto, JAPAN.

[6] J. Kaneda, S. Kasahara, J. Kuniya, K. Moriya, F. Kano, N. Saito, A. Shioiri, T. Shibayama, and H. Takahashi, "General Corrossion Properties of Titanium Based Alloys for the Fuel Claddings in the Supercritical Water-cooled Reactor," 12th International Conference on Environmental Degradation of Materials in Nuclear Power Systems-Water Reactor, August 15-18, 2005, Salt Lake City, Utah.

[7] J. Kaneda, S. Kasahara, J, Kuniya, F. Kano, H. Takahashi, and H. Matsui, "Material Properties of Stainless Steels Modified with Addition of Zirconium for Supercritical Water-Cooled Reactor ," Proc.ICAPP'07, Paper 7500, Nice, France, 2008.

[8] H. Matsui, Y. Sato, N. Saito, F. Kano, K. Ooshima, J. Kaneda, K. Moriya, S. Ohtsuka, and Y. Oka, "Material Development for Supercritical Water-cooled Reactors," Proceedings of ICAPP 2007, Nice, France, Paper 7447, May 13-18, 2007.

[9] NIMS Creep Data Sheet, No. 6B, "Data Sheets on the Elevated-temperature Properties of 18Cr-12Ni-Mo Stainless Steel Tube for Boilers and Heat Exchangers (SUS 316H TB)"

[10] S. Kasahara, J.Kuniya, K. Moriya and F. Kano, S. Shiga and H. Takahashi, "Corrosion-Resistance of the Candidate Materials for the Fuel Claddings of the Supercritical Water Cooled Power Reactor", Proceedings of ICAPP'03, Cordoba, Spain, Paper 3293, May (2003).

[11] J. Kaneda, S. Kasahara, J. Kuniya, K. Moriya, F. Kano, N. Saito, A. Shioiri, T. Shibayama and H. Takahashi, " Corrosion Film Properties-of-the-Candidate Materials for the Fuel Claddings of the Supercritical-water Cooled Power Reactor", Proceedings of ICAPP'05, Seoul, Korea, Paper 5594, May (2005)

[12] Y. Maruno, J. Kaneda, S. Kasahara, N. Saito, T. Shikama, and H. Matsui, "Evaluation of Weight Loss of Stainless Steels in Supercritical Water," Proceedings of ICAPP 2009, Tokyo, Japan, Paper 9289, May 10-14, 2009

[13] Y. Tsuchiya, F. Kano, N. Saito, S. Shiga,S. Kasahara, K.Moriya, and H. Takahashi, “SCC and Irradiation Properties of Metals under Supercritical-water Cooled Power Reactor Conditions,” International Conference on Global Environment and Advanced Nuclear Power Plants (GENES4/ANP) Paper #1096 (2003.9.1, Kyoto).

[14] Tsuchiya, F. Kano, N. Saito, A. Shioiri, K. Moriya and S. Kasahara, “SCC Properties of Metals under Supercritical-water Cooled Power Reactor Conditions,” Corrosion2004, Paper 4485, (March 28–April 1, 2004, New Orleans, LA).

[15] F. Kano, Y. Tsuchiya, K, Oka, N. Saito, S. Mimura, S. Kasahara, J. Kaneda, H. Matsui, T. Shikama, M. Narui, and Y. Oka, “Thermal and Irradiation Effects on High-temperature Mechanical Properties of Materials for SCWR Fuel Cladding,” Proceedings of ICAPP ’09, Tokyo, Japan, Paper 9428, May 10-14, 2009.

[16] L. R. Greenwood, J. Nucl. Mater., 115(1983)137.

Table 1 The requirements for material tests.

| Required specifications | | |
|---|---|---|
| Categories | Data requirements | Conditions |
| Thermal property | Thermal expansion | Temperature: over 800˚C |
| Mechanical property | Yield strength (Sy)<br>Ultimate tensile strength (Su)<br>Elongation<br>Young's module (E)<br>Poisson ration ($\nu$)<br>Mayer hardness | Tensile test and hardness test<br>- non-irradiated<br>- irradiated<br>Temperature: up to 800˚C<br>-Normal: 300 - 700˚C<br>-Transient: less than 800˚C<br>Fluence: Fast N $2x10^{26}n/m^2$<br>Thermal N $8x10^{25}n/m^2$ |
| Fatigue | Damage curve | Tensile test<br>- non-irradiated<br>- irradiated<br>Temperature:<br>-Normal: 300 - 700˚C |
| Creep | Stress to rupture (Sr: LMP)<br>Creep rate | Inner pressure tube test<br>- non-irradiated<br>- irradiated<br>Pressure difference: up to 10MPa<br>Temperature: up to 800˚C<br>-Normal: 300 - 700˚C<br>-Transient: less than 800˚C<br>Time: over 6 years<br>Fluence: Fast N $2x10^{26}n/m^2$ |
| Dimension change | Irradiation swelling rate | Irradiation<br>Temperature: up to 800˚C<br>-Normal: 300 - 700˚C<br>-Transient: less than 800˚C<br>Load: up to 30MPa<br>Fluence: Fast N $2x10^{26}n/m^2$<br>Thermal N $8x10^{25}n/m^2$ |
| Corrosion | Thinning rate<br>Dissolution rate | Autoclave test (SCW)<br>Temperature: over 700˚C<br>Time: over 6 years |
| SCC | IGSCC fracture surface rate | Confirmation of immunity |
| PCCI | Reaction rate at inner | Confirmation of immunity |
| Embrittlement | Hydride (with SCW)<br>He-embrittlement | Confirmation issue<br>Fluence: Fast N $2x10^{26}n/m^2$<br>Thermal N $8x10^{25}n/m^2$ |
| Manufacturability | Cladding proceduction<br>Heat effect | Confirmation issue |

Table 2 Chemical compositions (wt.%) and thermal treatment of the test materials.

(a) Ferritic/Martensitic stees

| Alloy | C | Si | P | Ni | Cr | Fe | Mo | Others | Thermal Treatment |
|---|---|---|---|---|---|---|---|---|---|
| Mod. 9Cr-1Mo | 0.11 | 0.38 | 0.011 | 0.13 | 8.59 | Bal. | 0.95 | Nb: 0.084 | A) |
| 12Cr-1Mo-1WVNb | 0.11 | 0.23 | 0.018 | - | 11.97 | Bal. | 0.95 | Nb: 0.05, W: 0.99, V: 0.25 | B) |

(b) Austenitic stainless steels

| Alloy | C | Si | P | Ni | Cr | Fe | Mo | Others | Thermal Treatment |
|---|---|---|---|---|---|---|---|---|---|
| Type 304 | 0.04 | 0.59 | 0.028 | 8.3 | 18.17 | Bal. | - | | 1050°C x 30 min (WQ) |
| Type 316L | 0.023 | 0.67 | 0.028 | 12.21 | 17.57 | Bal. | 2.08 | | 1050°C x 30 min (WQ) |
| Type 310S | 0.05 | 0.70 | 0.016 | 19.17 | 25.19 | Bal. | - | | 1100°C x 30 min (WQ) |
| Type 316L+Zr (H1) | 0.006 | 0.46 | 0.016 | 10.71 | 16.54 | Bal. | 2.22 | Zr: 0.56 | 1150°C x 30 min (WQ) |
| Type 310S+Zr (H2) | 0.034 | 0.51 | 0.016 | 20.82 | 25.04 | Bal. | 0.51 | Zr: 0.59 | 1150°C x 30 min (WQ) |
| Fine Grain 310S (T3F) | 0.099 | 0.25 | <0.005 | 21.92 | 24.74 | Bal. | - | Ti: 0.81, N: 0.0006 | |
| Normal Grain 310S (T3N) | | | | | | | | | |
| Fine Grain 310S (T6F) | 0.092 | 0.25 | <0.005 | 22.81 | 25.03 | Bal. | 2.38 | Ti: 0.41, Nb: 0.26, N: 0.002 | |
| Normal Grain 310S (T6N) | | | | | | | | | |
| Fine Grain 310S (T7F) | 0.1 | 0.24 | <0.005 | 22.81 | 24.97 | Bal. | 2.04 | Ti: 0.42, Nb: 0.58 | |

(c) Ni-based alloys

| Alloy | C | Si | P | Ni | Cr | Fe | Mo | Others | Thermal Treatment |
|---|---|---|---|---|---|---|---|---|---|
| Alloy 825 | 0.01 | 0.10 | - | 40.99 | 22.92 | Bal. | 3.23 | Al: 0.12, Ti: 0.92, Cu: 1.97 | 1100°C x 30 min (WQ) |
| Hastelloy C(HC) 22 | 0.002 | 0.01 | <0.01 | Bal. | 21.50 | 4.5 | 13.4 | Co: 0.2, W: 3.0, V: 0.02 | 1120°C x 30 min (WQ) |
| Alloy 600 | 0.07 | 0.19 | - | 74.79 | 14.63 | 9.77 | - | Cu: 0.22 | 1100°C x 30 min (WQ) |
| Alloy 625 | 0.01 | 0.10 | 0.009 | 61.21 | 21.40 | 3.61 | 9.26 | Al: 0.19, Ti: 0.30, Nb+Ta: 3.76 | 1100°C x 30 min (WQ) |
| Alloy 690(SHT) | 0.02 | 0.33 | 0.01 | 59.05 | 29.45 | 10.3 | - | Cu: 0.02 | 1120°C x 30 min (WQ) |
| Alloy 718(Ordinary) | 0.04 | 0.08 | 0.003 | 53.2 | 17.90 | Bal. | 3.07 | Al: 0.53, Ti: 1.13,Co: 0.02, Cu: 0.01,Nb+Ta: 5.15, | F) |
| Alloy 718(Mod) | | | | | | | | | G) |

(d) Ti-based alloys

| Alloy | H | O | N | C | Fe | Al | V | Ti | Others | Thermal Treatment |
|---|---|---|---|---|---|---|---|---|---|---|
| Ti-6Al-4V | 0.0041 | 0.18 | 0.01 | 0.01 | 0.23 | 6.33 | 4.29 | Bal. | Y<0.001 | 750°Cx2 h (FC) |
| Ti-3AL-2.5V | 0.0026 | 0.11 | 0.005 | 0.08 | 0.23 | 3.05 | 3.00 | Bal. | - | 750°C C) |
| Ti-15V-3Al-3Sn-3Cr | 0.012 | 0.10 | 0.009 | - | 0.221 | 3.06 | 15.21 | Bal. | Sn 2.95 Cr 3.10 | D) |
| Ti-15Mo-5Zr-3Al | 0.01 | 0.12 | 0.01 | - | 0.03 | 3.30 | - | Bal. | Mo:14.7 Zr:4.8 | E) |

A): 1045°C x 30 min + 780°C x 1.5 h (AC)
B): 1050°C x 1 h (AC) + 800°C x 1 h
C): Annealing & Pickling
D): SHT 800°C x 20 min (AC) -> 510 °C x 14 h (AC)
E): SHT 735°C x 1 h (WQ) -> 500°C x 14 h (AC)
F): 1010°C x 1 h (WQ) +705°C x 6 h (AC)
G): 955°C x 1 h + 718°C x 8 h (FC)+ 621°C x 8 h (AC)
(WQ): Water Quench, (AC): Air Cooling, (FC): Furnace Cooling, (SHT):Solution Heat Treatment

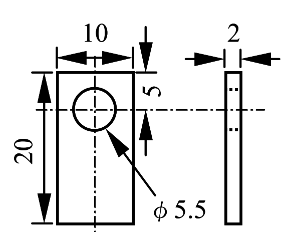


Figure 1 Diagram of the general corrosion test specimen (mm)

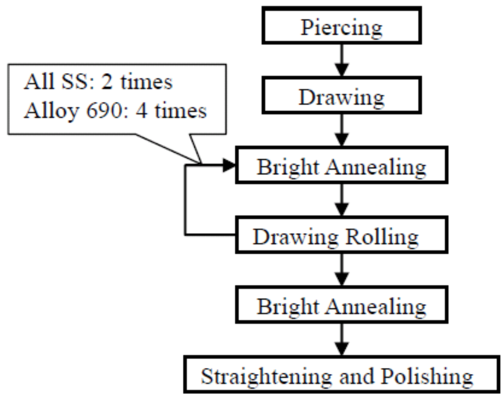


Figure 2 Manufacturing process of small-diameter thin-wall tube.

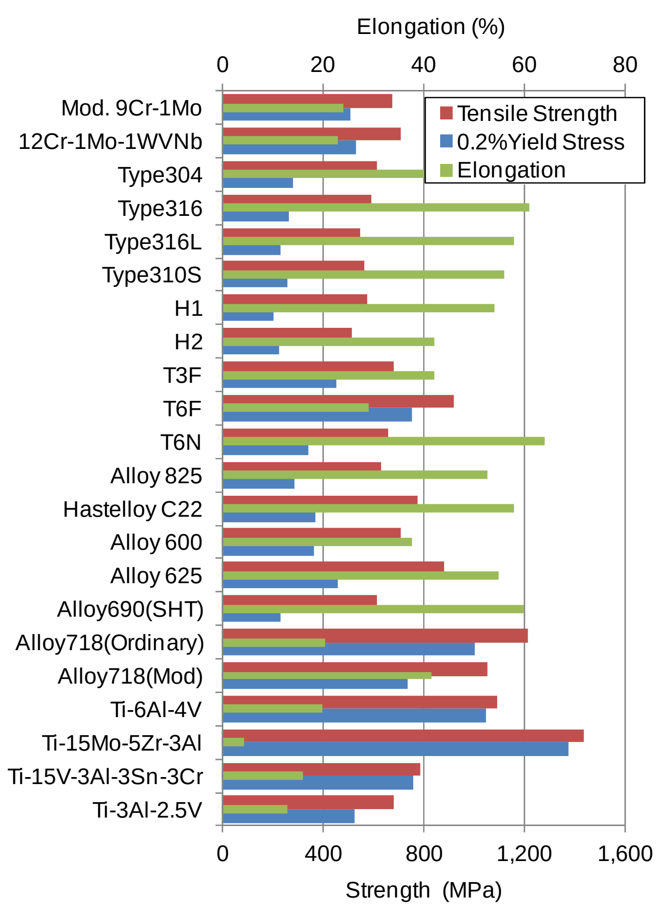


(a) Room temperature

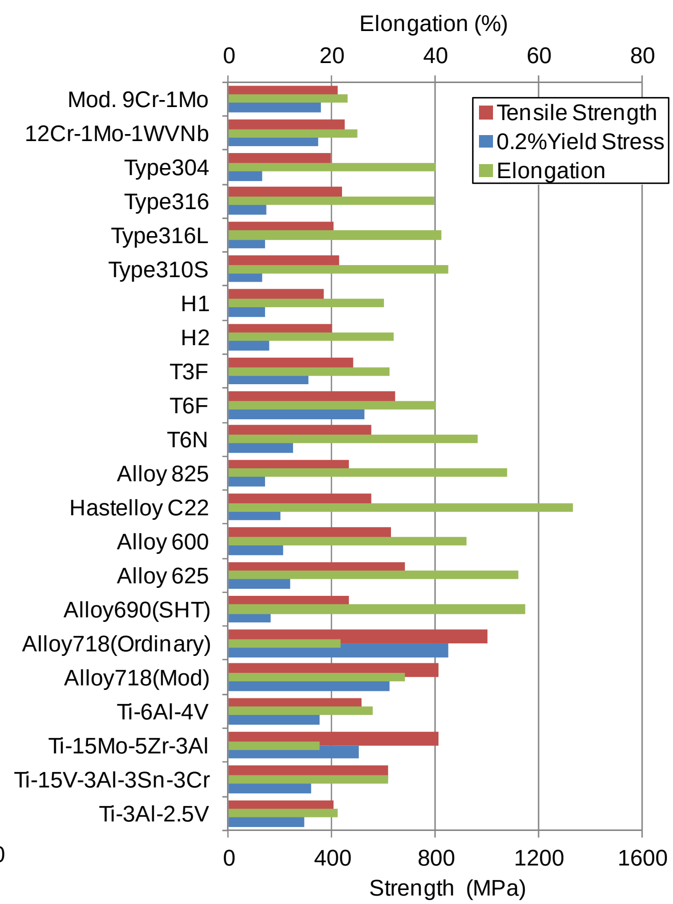


(b) 550˚C

Figure 3 Tensile properties of the test materials at room temperature and 550˚C

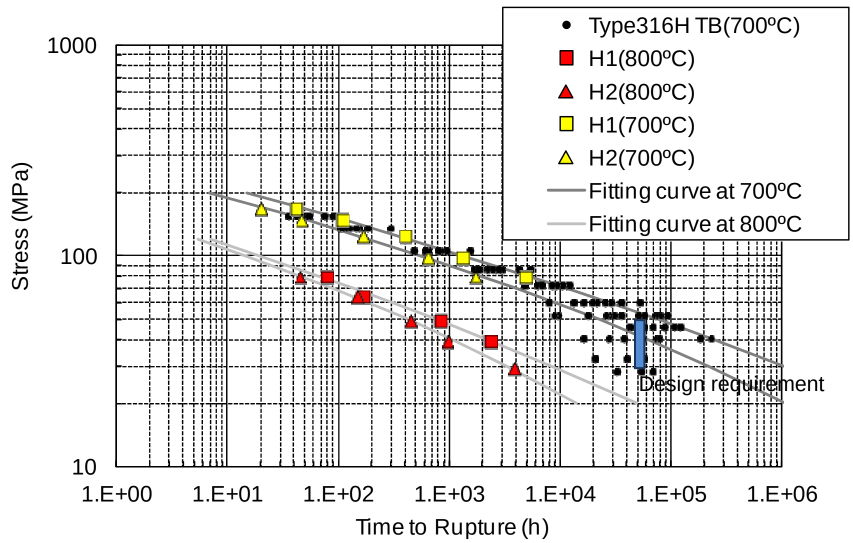


Figure 4 Stress versus time to rupture of H1, H2 and Type 316 at 700 and 800˚C.

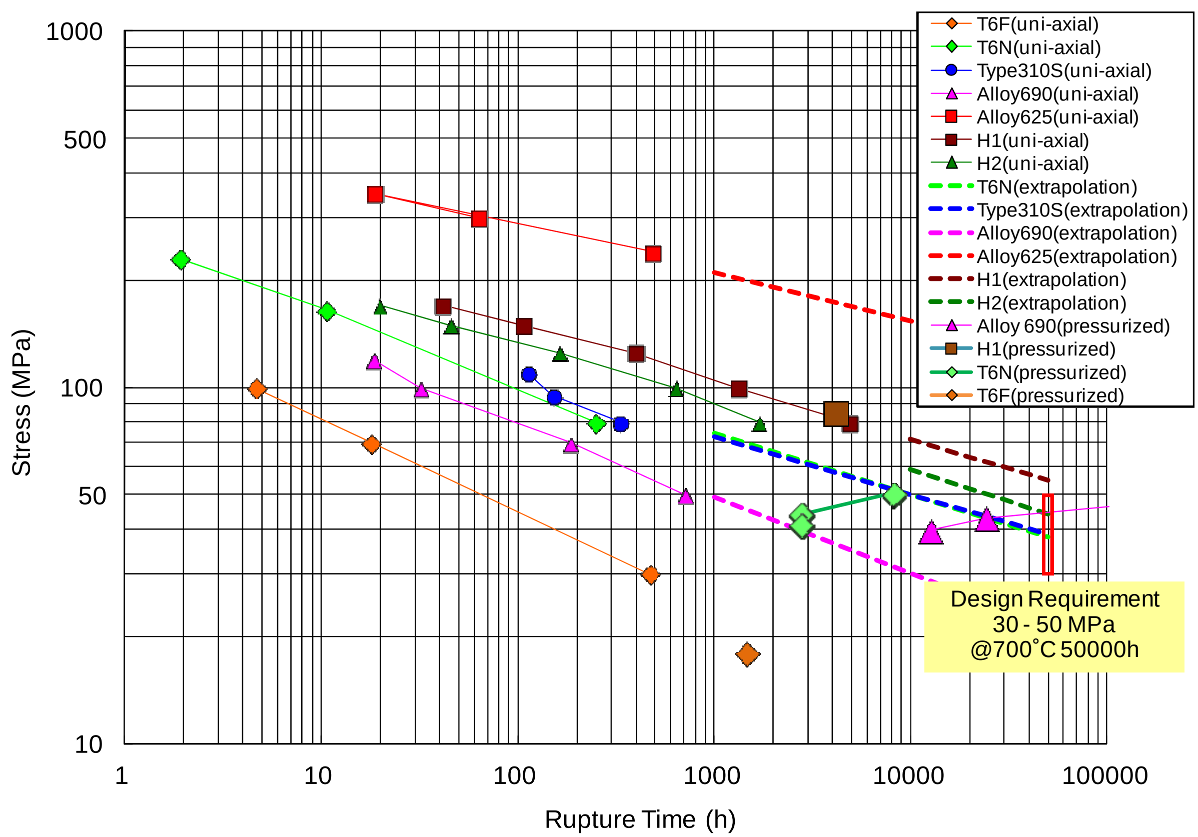


Figure 5 Thermal creep test results with uniaxial and pressurized tube methods at 700˚C.

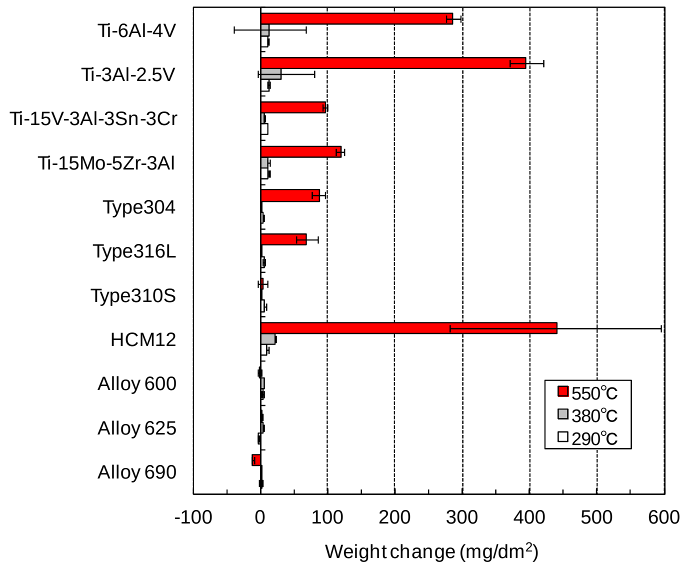


Figure 6 Weight change after supercritical water exposure for 500 h.

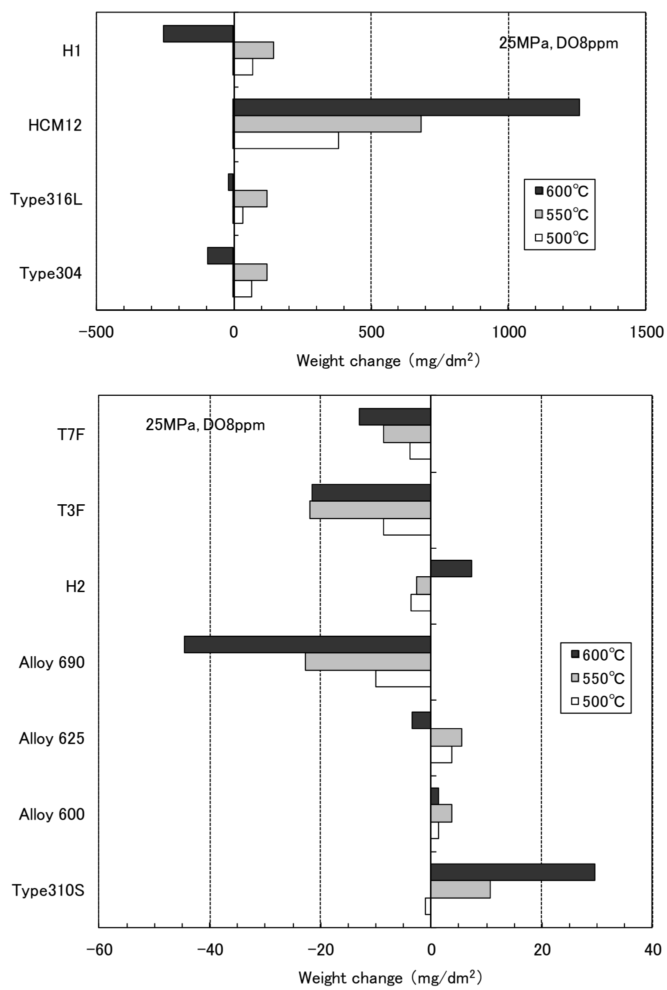


Figure 7 Weight change after supercritical water exposure at 500, 550 and 600˚C for 1000h.

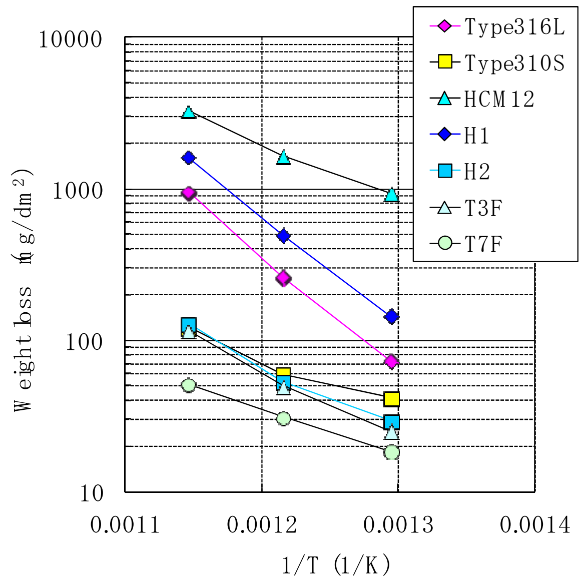


Figure 8 Arrhenius plots of weight loss of test materials

Table 3 Prediction results of depth of corrosion thinning under SCWR conditions.

| Material | Arrhenius plot | | | 700°C, 1,000h | | | 700°C, 50,000h |
|---|---|---|---|---|---|---|---|
| | | | | Weight loss (mg/dm²) | Specific gravity of material (g/cm³) | Depth of corrosion thinning (μm) | ∝ t^0.5 |
| | E (eV) | $A_0$ | $R^2$ | | | | Depth of corrosion thinning (μm) |
| SUS304 | 1.19 | 9.61E+09 | 0.9917 | 6380.0 | 7.93 | 80.5 | 568.9 |
| SUS316L | 1.39 | 1.35E+11 | 0.9908 | 8145.0 | 8.00 | 101.8 | 719.9 |
| SUS310S | 0.57 | 2.78E+05 | 0.9844 | 305.1 | 7.98 | 3.8 | 27.0 |
| 12Cr-1Mo-1WVNb | 0.73 | 5.57E+07 | 0.9947 | 9024.8 | 7.80 | 115.7 | 818.1 |
| H1 | 1.38 | 1.81E+11 | 0.9990 | 13124.1 | 8.00 | 164.1 | 1160.0 |
| H2 | 0.83 | 9.28E+06 | 0.9810 | 468.0 | 7.98 | 5.9 | 41.5 |
| T3 | 0.82 | 7.15E+06 | 0.9971 | 394.3 | 7.98 | 4.9 | 34.9 |
| T7 | 0.54 | 9.33E+04 | 0.9722 | 155.7 | 7.98 | 2.0 | 13.8 |

Table 4 SSRT results at 290 and 550°C.

| Test materials | | Fracture surface | |
|---|---|---|---|
| | | 290°C | 550°C |
| F/M steel | HCM12 | - | No SCC |
| Austenitic SS | Type 304 | IGSCC | No SCC |
| | Type 316L | No SCC | No SCC |
| | Type 310S | IGSCC | IGSCC |
| | H2 | No SCC | No SCC |
| | T6F | No SCC | No SCC |
| Ni-based alloy | Alloy 600 | No SCC | No SCC |
| | Alloy 625 | No SCC | IGSCC |
| | Alloy 690 | No SCC | No SCC |
| Ti-based alloy | Ti-15Mo-5Zr-3Al | No SCC | TGSCC |

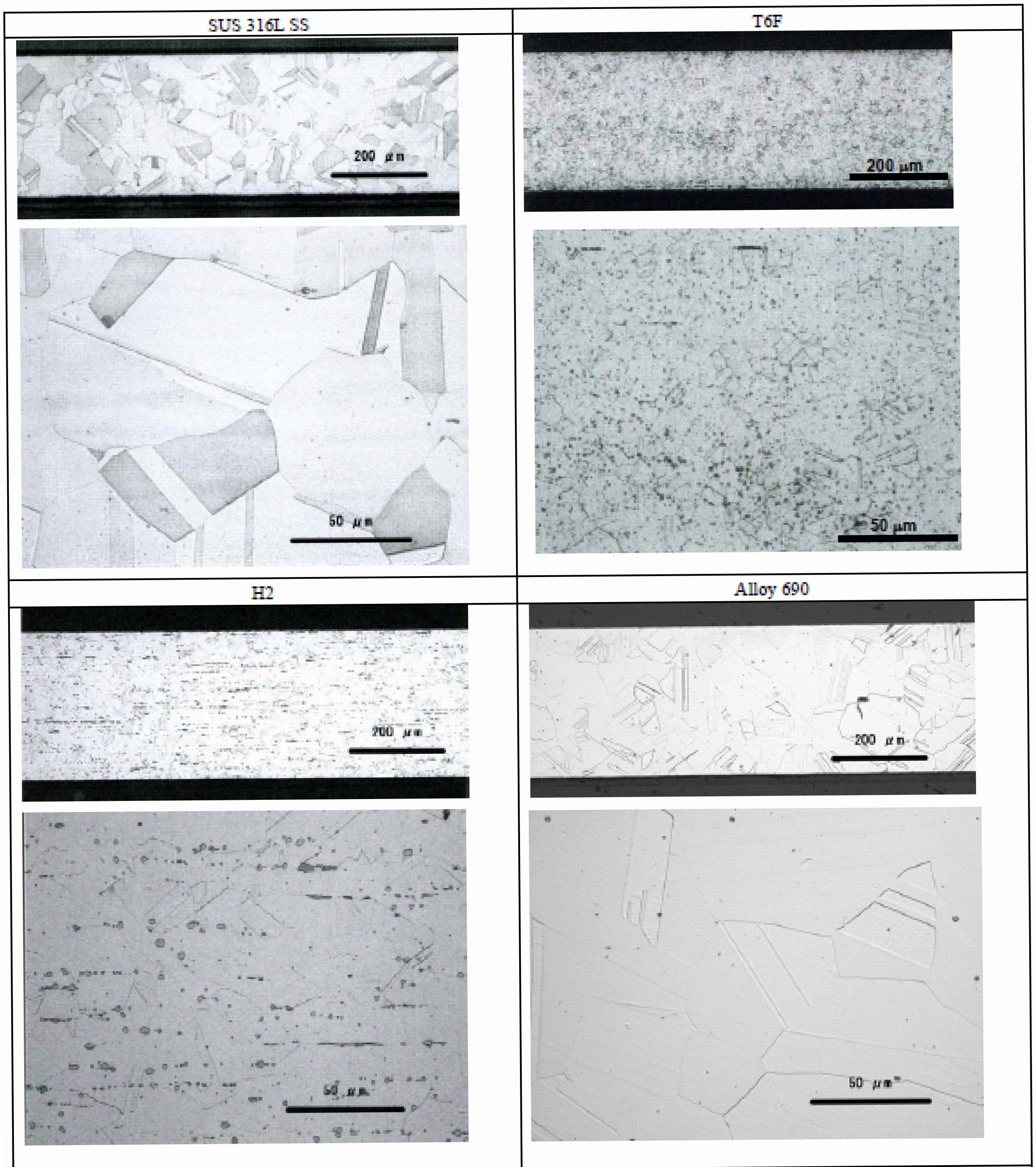


Figure 9 Microstructure of small-diameter thin-wall tube.

Table 5 Calculation results of He yield in candidate alloys (appm)

| Material (Ni at%) | Transmutation Reaction | | |
|---|---|---|---|
| | $^{58}Ni(n,\gamma)^{59}Ni(n,)^{56}Fe$ | $^{58}Ni(n,)^{55}Fe$ | $^{60}Ni(n,)^{57}Fe$ |
| Type 310S(18) | 105 | 17 | 2 |
| Type 316L (11) | 68 | 11 | 1 |
| Alloy 690 (58) | 338 | 56 | 5 |
| Pure Ni (100) | 583 | 96 | 9 |

| Materials | | Yield stress | Tensile strength | Elongation | Creep lifetime | General corrosion | SCC susceptibility | He embrittlement | Manufacturability | Comprehensive evaluation | |
|---|---|---|---|---|---|---|---|---|---|---|---|
| F/M steel | HCM12 | - | - | - | - | C | - | - | - | | |
| Austenitic stainless steels | Type 316L | A | A | A | A | C | A | A | A | | |
| | H1 | A | A | A | A | C | A | - | A | | |
| | Type 310S | A | A | A | A | A | B | A | A | B | 2nd candidate |
| | H2 | A | A | A | A | A | A | A | A | A | 1st candidate |
| | T3F | C | - | - | - | A | - | B | - | | |
| | T6F | C | - | - | C | A | A | B | A | | |
| | T6N | A | A | A | A | - | A | B | - | B | 2nd candidate |
| Ni based alloys | Alloy 600 | A | A | A | - | A | A | C | - | | |
| | Alloy 625 | A | A | A | A | A | B | C | A | | |
| | Alloy 690 | A | A | A | C | A | A | C | - | | |

A: Good, B: Fair, C: No good, -: N/A

Figure 10 Comprehensive evaluation of material applicability for the SCWR fuel cladding.